

# Limited induction of lung-resident memory T cell responses against SARS-CoV-2 by mRNA vaccination

Daan K.J. Pieren<sup>1</sup>, Sebastián G. Kuguel<sup>1</sup>, Joel Rosado<sup>2</sup>, Alba G. Robles<sup>1</sup>, Joan Rey-Cano<sup>1</sup>, Cristina Mancebo<sup>1</sup>, Juliana Esperalba<sup>3</sup>, Vicenç Falcó<sup>1</sup>, María J. Buzón<sup>1</sup>, Meritxell Genescà<sup>1\*</sup>

## Affiliations

<sup>1</sup> Infectious Diseases Department, Vall d'Hebron Institut de Recerca (VHIR), Vall d'Hebron Hospital Universitari, Vall d'Hebron Barcelona Hospital Campus, Passeig Vall d'Hebron 119-129, 08035 Barcelona, Spain;

<sup>2</sup> Thoracic Surgery and Lung Transplantation Department, Vall d'Hebron Institut de Recerca (VHIR), Vall d'Hebron Hospital Universitari, Vall d'Hebron Barcelona Hospital Campus, Passeig Vall d'Hebron 119-129, 08035 Barcelona, Spain;

<sup>3</sup> Respiratory Viruses Unit, Microbiology Department, Vall d'Hebron Institut de Recerca (VHIR), Vall d'Hebron Hospital Universitari, Vall d'Hebron Barcelona Hospital Campus, Passeig Vall d'Hebron 119-129, 08035 Barcelona, Spain.

## Corresponding author:

Meritxell Genescà  
Vall d'Hebron Research Institute (VHIR)  
Infectious Disease Department  
119-129 Passeig Vall d'Hebron, 08035 Barcelona, Spain  
Phone: +34 93 274 6200  
Email: [meritxell.genesca@vhir.org](mailto:meritxell.genesca@vhir.org)

36 **Abstract**

37 Resident memory T cells ( $T_{RM}$ ) present at the respiratory tract may be essential to enhance early  
38 SARS-CoV-2 viral clearance, thus limiting viral infection and disease. While long-term antigen  
39 (Ag)-specific  $T_{RM}$  are detectable beyond 11 months in the lung of convalescent COVID-19 patients  
40 after mild and severe infection, it is unknown if mRNA vaccination encoding for the SARS-CoV-2  
41 S-protein can induce this frontline protection. We found that the frequency of  $CD4^+$  T cells  
42 secreting interferon ( $IFN$ ) $_{\gamma}$  in response to S-peptides was variable but overall similar in the lung  
43 of mRNA-vaccinated patients compared to convalescent-infected patients. However, in  
44 vaccinated patients, lung responses presented less frequently a  $T_{RM}$  phenotype compared to  
45 convalescent infected individuals and polyfunctional  $CD107a^+ IFN_{\gamma}^+ T_{RM}$  were virtually absent.  
46 Thus, a robust and broad  $T_{RM}$  response established in convalescent-infected individuals may be  
47 advantageous in limiting disease if the virus is not blocked by initial mechanisms of protection,  
48 such as neutralization. Still, mRNA vaccines might induce responses within the lung parenchyma,  
49 potentially contributing to the overall disease control.

## 50 Introduction

51 The COVID-19 pandemic continues, and many countries face multiple resurgences. While  
52 vaccines to limit SARS-CoV-2 infection rapidly emerged providing high protection from COVID-  
53 19, more insight into the mechanisms of protection induced by available vaccines is still needed.  
54 The level of vaccine-induced neutralizing antibodies has been shown to correlate with protection  
55 from symptomatic infection; however, predicted antibody-mediated vaccine efficacy declines over  
56 time <sup>1</sup>. Moreover, many viral variants of concern (VOC) can significantly evade humoral immunity,  
57 yet cellular responses induced by vaccines show strong cross-protection against these variants <sup>2</sup>.  
58 <sup>3</sup>, supporting the idea that cellular responses largely contribute to disease control <sup>4</sup>. In fact,  
59 preexisting cross-reactive memory T cells and early Nucleocapsid (N) responses against  
60 coronaviruses are associated with protection from SARS-CoV-2 infection <sup>5, 6</sup>.  
61 Further, SARS-CoV-2 infection induces robust cellular immunity detectable beyond 10 months  
62 after infection in peripheral blood <sup>7</sup>, and as T<sub>RM</sub> in the lung <sup>8</sup>, and the number of SARS-CoV-2-  
63 specific T<sub>RM</sub> in the lung correlates with clinical protection <sup>9</sup>. Vaccination against SARS-CoV-2  
64 using BTN162b2 (Pfizer/BioNTech) and mRNA-1273 (Moderna) vaccines has been reported to  
65 induce CD4<sup>+</sup> and CD8<sup>+</sup> T-cell responses in peripheral blood <sup>10, 11</sup>. Moreover, the IFN $\gamma$  T-cell  
66 response to SARS-CoV-2 S-peptides, one of the main antiviral factors measured as a readout,  
67 further increased after boosting <sup>11</sup>. However, current studies only address vaccine-induced SARS-  
68 CoV-2 specific T-cell responses in peripheral blood and whether mRNA vaccines also elicit  
69 SARS-CoV-2-specific long-term T<sub>RM</sub> cells in the lung remains to be established.

70 To this end, we determined the presence of SARS-CoV-2-specific CD4<sup>+</sup> and CD8<sup>+</sup> T cells  
71 in 26 paired peripheral blood and lung cross-sectional samples from: I.) uninfected unvaccinated  
72 individuals (Ctrl, n=5), II.) unvaccinated long-term SARS-CoV-2 convalescent individuals (Inf,  
73 n=9, convalescent for a median of 304 days [183-320 IQR]), III.) uninfected and long-term two-  
74 dose vaccinated individuals (Vx2, n=7, a median of 206 days [184-234] after the second dose),

75 and IV.) uninfected and short-term three-dose vaccinated individuals (Vx3, n=5, a median of 52  
76 days [42-54] after the third dose or boost). Whereas our data showed that S-specific T cells can  
77 be detected in the lung of mRNA-vaccinated individuals up to 8 months after immunization, lung  
78 responses in vaccinated patients presented less frequently a T<sub>RM</sub> phenotype and polyfunctional  
79 T<sub>RM</sub> expressing IFN $\gamma$  and CD107a were essentially absent compared to convalescent patients.

80

81

82

83

84

85

86

87

88

89

90

91

92

93

94

95

96

97

98

99

100

101 **Results**

102 **Cohort characteristics**

103 Paired cross-sectional peripheral blood and healthy tissue areas obtained from patients  
104 undergoing lung resection for differing oncologic reasons were studied. Patient characteristics are  
105 summarized in Supplemental Table 1. In order to confirm the SARS-CoV-2 status of each patient,  
106 we analyzed total immunoglobulin (Ig) or IgG levels against N and Spike (S) proteins respectively,  
107 which discriminated Ctrl (negative for N and S), Inf patients (positive for N and S) and vaccinated  
108 groups (negative for N and positive for S; Supplemental Table 1). Furthermore, the viral  
109 neutralization titer was determined against the SARS-CoV-2 Omicron variant using a pseudovirus  
110 neutralization assay and, as expected<sup>10, 11</sup>, a positive correlation between neutralization and S-  
111 IgG titers was detected (Spearman  $r = 0.72$ ,  $P = 0.0016$ ; Supplemental Figure 1A). In addition to  
112 the absence of neutralization of the Omicron variant in plasma of the Ctrl group, 2 out of 7 patients  
113 (28%) in the Inf group and from 1 out of 6 patients (17%) in the Vx2 group failed to neutralize the  
114 virus, whereas all patients in the Vx3 group were able to neutralize this variant (Supplemental  
115 Table 1). The fact that we mostly studied elderly patients could certainly determine the overall  
116 response and, indeed there was a negative correlation between older age and neutralizing  
117 capacity for the Inf group (Spearman  $r = -0.88$ ,  $P = 0.01$ ; Supplemental Figure 1B) and the same  
118 trend was observed for the Vx2 group (Spearman  $r = -0.72$ ,  $P = 0.10$ ; Supplemental Figure 1C).  
119 This relationship was less evident between age and S-IgG titers (Supplemental Figure 1D, E), yet  
120 examples in larger cohorts exist<sup>10</sup>. Instead, S-IgG titers from all groups negatively correlated with  
121 sample timing (Spearman  $r = -0.61$ ,  $P = 0.010$ ; Supplemental Figure 1F), a correlation that was  
122 also observed for total Ig against N in the Inf group (Spearman  $r = -0.88$ ,  $P = 0.009$ ; Supplemental  
123 Figure 1G), which agrees with antibody titers decay<sup>10, 11, 12</sup>.

124

125

126 **Recent mRNA booster vaccination elicits S-specific CD4<sup>+</sup> T cells similar to convalescent**  
127 **infection**

128 To address cellular immune responses, we stimulated fresh peripheral blood mononuclear cells  
129 (PBMC) and lung-derived cellular suspensions with overlapping Membrane (M), N and S peptide  
130 pools and determined the intracellular expression of IFN $\gamma$ , interleukin (IL)-4, and IL-10, along with  
131 the degranulation marker CD107a in CD4<sup>+</sup> and CD8<sup>+</sup> T cells (Supplemental Figure 2A), as  
132 previously described <sup>8</sup>. We found detectable circulating IFN $\gamma$ -secreting Ag-specific CD4<sup>+</sup> T cells  
133 responding to all proteins in the blood of Inf patients, which was significantly higher compared to  
134 the Ctrl, Vx2, and Vx3 groups for M and N peptides (Figure 1A, B). In contrast, for S peptides, the  
135 Inf group only showed higher frequencies of IFN $\gamma$ <sup>+</sup> CD4<sup>+</sup> T cells compared to the Ctrl group,  
136 indicating an increase induced by vaccination in the blood of Vx2 and Vx3 groups. However, only  
137 two Vx2 patients showed detectable frequencies of S-specific CD4<sup>+</sup> T cells in blood, while recently  
138 boosted Vx3 patients displayed an overall increase reaching statistical significance compared to  
139 the Ctrl group (Figure 1B). In contrast to CD4<sup>+</sup> T cells, the frequencies of IFN $\gamma$ <sup>+</sup> CD8<sup>+</sup> T cells  
140 detected were minimal for each of the groups against any of the proteins, including for the Vx  
141 groups against S peptides (Figure 1B). Expression of IL-4, IL-10, and CD107a by T cells showed,  
142 in general, high variability, limiting the detection of differences (Supplemental Figure 3).  
143 Nonetheless, S-specific degranulating CD107a<sup>+</sup> CD8<sup>+</sup> T cells were overall more frequent in the  
144 Vx2 compared to the Ctrl group ( $P = 0.046$ ; Supplemental Figure 3). Together, these data indicate  
145 that M, N, and S-peptide specific IFN $\gamma$ <sup>+</sup> CD4<sup>+</sup> T cell responses can be readily detected in blood  
146 months after resolving natural SARS-CoV-2 infection and that these responses require a recent  
147 mRNA vaccine booster-dose against SARS-CoV-2 to elicit similar frequencies against the S  
148 protein in vaccinated individuals.

149

150

151 **mRNA vaccination induces S-specific CD4<sup>+</sup> T cells in the lung**

152 As reported previously <sup>8</sup>, we here found that mild or severe natural infection with SARS-CoV-2  
153 induced robust IFN $\gamma$ <sup>+</sup> CD4<sup>+</sup> T cells in the lung against M, N, and S peptides, detectable for up to  
154 12 months after infection (Figure 2A, B). Interestingly, whereas M and N-specific IFN $\gamma$ <sup>+</sup> CD4<sup>+</sup> T-  
155 cell frequencies were significantly higher in the Inf group compared to Ctrl or Vx groups, these  
156 differences were not observed for S-specific responses (Figure 2A, B). Vx2 and Vx3 groups  
157 showed presence of S-specific IFN $\gamma$ <sup>+</sup> CD4<sup>+</sup> T cells in the lung in most patients and its frequency  
158 was comparable to levels detected in Inf patients, although statistical significance was not reached  
159 compared to the Ctrl group (Figure 2B). In contrast to CD4<sup>+</sup> T cells, CD8<sup>+</sup> T cells producing IFN $\gamma$   
160 after stimulation with M, N, or S peptides was variable within each group and did not result in  
161 significant differences between the groups, indicating that natural infection nor vaccination elicit  
162 a robust IFN $\gamma$  positive CD8<sup>+</sup> T cell response in the human lung (Figure 2B). Furthermore, induction  
163 of lung anti-SARS-CoV-2-specific T-cell responses involving expression of IL-4, IL-10, and  
164 CD107a did not differ between groups (Supplemental Figure 4A). Of note, in this tissue  
165 compartment, we detected negative correlations between patient's age within the Inf group and  
166 the frequency of S-specific degranulating CD4<sup>+</sup> and CD8<sup>+</sup> T cells (Spearman  $r = -0.76$ ,  $P = 0.024$   
167 and Spearman  $r = -0.77$ ,  $P = 0.020$  respectively, Supplemental Figure 4B).

168 When we compared the magnitude of S-specific T cells in paired blood and lung samples,  
169 we found increased frequencies of IFN $\gamma$ <sup>+</sup> CD4<sup>+</sup> T cells in the lungs of patients from the Inf group  
170 compared to blood ( $P = 0.039$ , Figure 2C). The same trend was observed for the Vx individuals,  
171 which was close to significant if both groups were pooled ( $P = 0.054$ ), although this increase was  
172 more variable as only 7 out of 12 Vx patients showed an increase, in contrast to 8 out of 9 Inf  
173 patients. In contrast, the CD8<sup>+</sup> T-cell compartment did not show clear differences between these  
174 two compartments (Figure 2C), neither any of the T-cell subsets for any other function, which  
175 were highly variable (Supplemental Figure 5). Together our data indicates that S-specific CD4<sup>+</sup>

176 T-cell responses are detectable in the lung of uninfected vaccinated patients, suggesting that  
177 mRNA vaccination against SARS-CoV-2 may potentially elicit tissue-localized protective T-cell  
178 responses already after the second mRNA vaccine dose.

179

### 180 **Limited induction of tissue resident memory T cells by mRNA vaccination**

181 Presence of T<sub>RM</sub> cells may provide a better correlate of protection from disease in SARS-CoV-2  
182 infected individuals and are characterized by expression of CD69 and/or CD103<sup>8,9</sup>. Moreover,  
183 T<sub>RM</sub> cells require downregulation of the transcription factor T-bet for expression of CD103 and  
184 their formation and survival at tissue sites<sup>13</sup>. In order to assess if S-specific T cell responses  
185 detected in Vx patients had indeed a T<sub>RM</sub> phenotype, we analyzed expression of CD69 and CD103  
186 by lung SARS-CoV-2-specific CD4<sup>+</sup> and CD8<sup>+</sup>T cells, which we classified as: CD69<sup>-</sup> (non-T<sub>RM</sub>),  
187 CD69<sup>+</sup> (T<sub>RM</sub>) and a subset within CD69<sup>+</sup> cells expressing CD103<sup>+</sup> (T<sub>RM</sub> CD103<sup>+</sup>) (Figure 3A,  
188 Supplemental Figure 2B for gating strategy). Additionally, we assessed expression of T-bet to  
189 assure that CD69 in the lung was associated to a T<sub>RM</sub> phenotype and not to activation of CD69<sup>-</sup> T  
190 cells or the product of residual blood in the lung. Both CD69<sup>+</sup> T<sub>RM</sub> and CD103<sup>+</sup> T<sub>RM</sub> subsets did  
191 not show T-bet expression across all patient groups, whereas a fraction of CD69<sup>-</sup> non-T<sub>RM</sub> cells  
192 presented T-bet expression (Supplemental Figure 2B), suggesting the association to tissue  
193 residency when absent<sup>8</sup>. S-specific CD4<sup>+</sup> T cells from the Inf group showed higher frequencies  
194 of IFN $\gamma$ <sup>+</sup> cells within the CD69<sup>+</sup> and CD103<sup>+</sup> T<sub>RM</sub> phenotypes (Figure 3A, B), with statistical  
195 significance reached for the overall CD69<sup>+</sup> T<sub>RM</sub> fraction compared to the non-T<sub>RM</sub> fraction.  
196 Furthermore, while no significant differences were detected for CD103<sup>+</sup> T<sub>RM</sub> cells against S-  
197 peptides in any of the groups, a trend was observed for CD4<sup>+</sup> T-cell responses to M peptides and  
198 statistical significance was reached for CD8<sup>+</sup> T cells against N peptides compared to the non-T<sub>RM</sub>  
199 fraction in the Inf group (Supplemental Figure 6A, B). Of note, a negative correlation was observed  
200 between IFN $\gamma$ -secreting S-specific CD8<sup>+</sup> CD103<sup>+</sup> T<sub>RM</sub> cells and sample timing (Spearman  $r = -$



201 0.82,  $P = 0.019$  Supplemental Figure 6C). In addition, some patients in the Vx2 and Vx3 groups  
202 showed modest presence of S-specific  $T_{RM}$  with or without CD103 expression in their lungs  
203 (Figure 3A, B). However, this response was highly heterogeneous and not statistically significant.  
204 These findings indicate that mRNA vaccination against SARS-CoV-2 can induce S-specific  $T_{RM}$   
205 in some, but not all individuals and may also last long term after the second vaccination.

206

### 207 **Overall functional T-cell response of lung and blood compartments**

208 To better gain insight into the overall S-specific response by each group, including all functions  
209 and considering lung- $T_{RM}$  phenotypes, we represented S-specific  $CD4^+$  and  $CD8^+$  T cell subsets  
210 as donut charts displaying the mean frequency of responses including all individuals (responders  
211 and non-responders, Figure 4). This way, a dominance of  $IFN\gamma$ -secreting  $CD4^+$  T cells was  
212 particularly associated to the two  $T_{RM}$  phenotypes in the Inf and, to a lesser extent, in the Vx2  
213 patients (Figure 4A). Further, S-specific responses within non- $T_{RM}$  and blood  $CD4^+$  T cells were  
214 functionally similar and in general dominated by  $IFN\gamma$  and IL-4 secretion (Figure 4A). In contrast,  
215 degranulation characterized the majority of lung S-specific  $CD8^+$  T cells from Inf individuals  
216 (Figure 4B), which correlated negatively with older age for the  $T_{RM}$  fractions (Spearman  $r = -0.88$ ,  
217  $P = 0.006$  for both CD103 positive and negative, Supplemental Figure 6D). Degranulation was  
218 also the major function in blood from the two Vx groups (Figure 4B). Last, in general,  $CD8^+$  T-cell  
219 responses considering all functions were of higher magnitude in long-term Vx2 individuals,  
220 reaching statistical significance for blood responses in comparison to the Ctrl group, as shown in  
221 the adjoin graph on the right (Figure 4B).

222

### 223 **Polyfunctional S-specific $IFN\gamma^+CD107a^+ CD4^+$ T cells are absent in vaccinated patients**

224 We previously detected a low but consistent polyfunctional  $IFN\gamma^+CD107a^+$  T-cell response mostly  
225 associated to the  $T_{RM}$  fraction in convalescent infected patients <sup>8</sup>. We therefore investigated

226 whether mRNA vaccination against SARS-CoV-2 would also induce such S-specific  
227 polyfunctional responses in both compartments (Figure 5A, B). Indeed, increased frequencies of  
228 polyfunctional IFN $\gamma$ <sup>+</sup>CD107a<sup>+</sup> CD4<sup>+</sup> T cells were detected in blood from the Inf group against N  
229 peptides compared to the Ctrl group, but not against M- and S-peptides. Interestingly, a trend  
230 towards higher frequencies of S-specific polyfunctional CD4<sup>+</sup> T cells was observed for the Vx3  
231 group (Figure 5A). Likewise, circulating polyfunctional S-specific CD8<sup>+</sup> T cells were enhanced in  
232 Vx2 individuals compared to Ctrl group (Figure 5A). In fact, if Vx groups were pooled to increase  
233 sample size, then both CD4<sup>+</sup> and CD8<sup>+</sup> T cells reached significance compared to Ctrl samples ( $P$   
234 = 0.037 for CD4<sup>+</sup> and  $P$  = 0.024 for CD8<sup>+</sup>). In addition, the frequency of polyfunctional  
235 IFN $\gamma$ <sup>+</sup>CD107a<sup>+</sup> cells present in total CD4<sup>+</sup> and CD8<sup>+</sup> T cells in the lung were only consistently  
236 increased in the Inf group against N peptides compared to the Ctrl and Vx3 groups (Figure 5B).  
237 Nevertheless, while a high degree of variability was observed among vaccinated patients,  
238 polyfunctional S-specific T cells were detected in some individuals (Figure 5B). Strikingly, S-  
239 specific CD4<sup>+</sup> polyfunctional CD103<sup>+</sup> T<sub>RM</sub> cells were virtually absent in the Vx2 and Vx3 groups,  
240 while being frequently present in the lungs of patients from the Inf group (Figure 6). Furthermore,  
241 the frequency of S-specific polyfunctional CD4<sup>+</sup> T cells in the CD69<sup>+</sup> T<sub>RM</sub> cells was higher in the  
242 Inf group compared to the Ctrl and Vx2 groups (Figure 6). Together, these data indicate that both  
243 short- and long-term vaccination do not induce S-specific IFN $\gamma$ <sup>+</sup>CD107a<sup>+</sup> CD103<sup>+</sup> T<sub>RM</sub> cells in the  
244 lung, which may contribute to antiviral activity.

245

#### 246 **Anti-SARS-CoV-2 T cell response dynamics in two cases of interest**

247 Last, considering the uniqueness of analyzing immune responses in paired blood and lung  
248 parenchyma samples and recent studies detailing changes in T cell responses in infected  
249 individuals already vaccinated and vice versa <sup>14</sup>, we highlight two patients that were discarded  
250 due to not fitting inclusion criteria, yet bring interesting data to the study. HL174 was a patient in

251 their fifties who received the third mRNA-1273 vaccine boost and, five days after, tested positive  
252 by PCR. We analyzed paired tissue samples 30 days after the boost/infection event  
253 (Supplemental Figure 7A). This patient had a neutralization titer of 1740 IU/mL against omicron,  
254 and had detectable IgG and Ig titers against S and N proteins (>800 AU/mL and 1.23 index,  
255 respectively). When comparing T-cell responses from blood and lung tissue, a much higher IFN $\gamma$ -  
256 response was observed in the lung, in particular against the N protein, which already contained  
257 responding cells with a T<sub>RM</sub> phenotype (Supplemental Figure 7B, C). In contrast, in blood,  
258 degranulation was enhanced mostly against S but also M protein and some proportion of IL-10  
259 secretion was detected against all proteins (Supplemental Figure 7B).

260 On the other hand, patient HL162, who was in their early seventies, was first infected  
261 presenting a mild COVID-19 and, several months after, received three doses of the mRNA-1273  
262 vaccine. In this case, we obtained samples 3.7 months after infection and another one 1.3 months  
263 after the third dose (due to a second intervention for a lung carcinoma), which corresponded to a  
264 year after initial infection, as shown (Supplemental Figure 8A). Neither of these two time points  
265 showed neutralization titers against omicron and the titers of IgG, instead of increasing after triple  
266 vaccination, decreased from 156 to 0 index for the N protein and from 306.54 to 13.85 AU/mL for  
267 S protein. The comparison of the tissue compartments after infection and after triple vaccination  
268 evidenced a concomitant strong decrease in T-cell responses in blood and tissue (Supplemental  
269 Figure 8B, C, and Supplemental Figure 9A, B). However, IFN $\gamma$ -secreting SARS-CoV-2 T cells  
270 against M and N proteins in the lung were better preserved from the original infection one year  
271 later than were responses against the S protein enhanced due to vaccination (Supplemental  
272 Figure 8B, C and Supplemental Figure 9A, B). Thus, while the lower respiratory tract compartment  
273 more faithfully represented T<sub>RM</sub> responses established already during the infection event one year  
274 earlier, responses in blood mostly vanished.

275

276 **Discussion**

277 Comprehensive studies comparing the magnitude and duration of the T cell responses indicate  
278 similar magnitude after dual vaccination and after natural SARS-CoV-2 infection <sup>4, 11, 14</sup>. However,  
279 these results may not hold if we consider that the magnitude, the functional profile and even the  
280 duration of these responses in blood may not faithfully reflect responses in the respiratory tract <sup>6,</sup>  
281 <sup>8, 9, 15</sup>. In fact, the individual comparison between these two compartments among the S-  
282 responding T cells from the different groups showed higher magnitude in the lung than in the  
283 blood, but also a different profile. A key difference, and the main driver of our study, was the  
284 establishment of long-term protection potentially mediated by T<sub>RM</sub> after vaccination, since  
285 longevity of SARS-CoV-2 T cell responses remains a critical question <sup>6</sup>. In principle, T<sub>RM</sub> are  
286 established by mucosal infection since Ag together with local signals promote the recruitment and  
287 establishment of this memory response. In this sense, intramuscular vaccination with an  
288 adenovector vaccine in mice did not induce SARS-CoV-2-specific T<sub>RM</sub> in their lungs <sup>16</sup>. Thus, to  
289 induce potent resident immunity, vaccine strategies may need to either use live-attenuated Ag or  
290 employ mucosal routes. Consequently, the absence of vaccine induced S-specific T<sub>RM</sub> could be  
291 expected in infection-naïve individuals. Still, recent data shows that a secretory IgA response was  
292 induced in ~30% of participants after two doses of a SARS-CoV-2 mRNA vaccine which, in  
293 addition, may play an important role in protection against infection <sup>15</sup>. While we detected S-specific  
294 IFN $\gamma$ <sup>+</sup> CD4<sup>+</sup> T cell responses in the lung of vaccinated individuals, the proportion of these cells in  
295 the T<sub>RM</sub> phenotype was modest, in particular if considering CD103 expression. Further, the  
296 presence of polyfunctional IFN $\gamma$ <sup>+</sup>CD107a<sup>+</sup>CD4<sup>+</sup>CD103<sup>+</sup>T<sub>RM</sub> appeared to be restricted to the lungs  
297 of convalescent-infected patients only, while absent in the lungs of vaccinated patients.

298 Another difference in the comparison of the cellular immunity between SARS-CoV-2-  
299 infected convalescent and uninfected-vaccinated individuals is the broader and potentially  
300 stronger response induced by symptomatic infection. This is partially manifested by the fact that

301 the overall magnitude of responses against M and N peptides are frequently higher than S  
302 peptides <sup>8, 17, 18, 19</sup>. Of note, disease severity may impact both the magnitude and function of the T  
303 cell response against the different proteins <sup>8, 20, 21</sup>. In addition, among other factors, age also  
304 influences the magnitude and duration of immune responses in distinct tissue compartments,  
305 even the establishment of T<sub>RM</sub> <sup>22</sup>, a factor that influenced the frequency of degranulation in the  
306 lung of our Inf patients, including within the T<sub>RM</sub> fraction. Yet advanced age will also limit the  
307 immune response to vaccination <sup>23</sup>. On the other hand, we have observed that different proteins  
308 induce different functional profiles during acute infection, which may influence disease control <sup>8</sup>.  
309 S-specific immune responses may better support B cell and antibody generation via follicular  
310 helper T cells, which are instrumental to limiting infection <sup>4, 8</sup>. Instead, responses against the N  
311 protein seem to more consistently induce polyfunctional antiviral T cells and these responses may  
312 be more conserved among other coronaviruses <sup>5, 8, 24, 25</sup>. Indeed, preexisting SARS-CoV-2 specific  
313 T cell responses have been found in the blood of unexposed individuals <sup>18, 26</sup>. In this sense, in our  
314 study we detected a low level of preexisting T cell responses in our control group mostly located  
315 in the lung, which may be in agreement with a recent report in tonsillar tissue <sup>27</sup>. Thus, another  
316 conclusion would be highlighting the interest of including other proteins beyond the spike such as  
317 N sequences, which has been suggested before <sup>5, 8, 19, 25, 28</sup>. Last, in terms of duration, our study  
318 lacks longitudinal data to assess the dynamics in the different compartments, yet it is assumed  
319 that T<sub>RM</sub> phenotypes will contribute to long-term persistence <sup>6, 8, 29</sup>. In fact, the only patient for  
320 which we had longitudinal sampling after infection and after the third vaccine boost (Supplemental  
321 Figure 8) demonstrated that even if vaccination fails to induce a systemic antibody response, a  
322 low frequency SARS-CoV-2 T cell response directed to proteins from the original infection  
323 remains exclusively detectable in the lung as T<sub>RM</sub> one year after.

324 The overall CD8<sup>+</sup> T cell response was enhanced in some but not all vaccinated patients  
325 and was in general low and dominated by degranulation. In fact, lung S-specific CD8<sup>+</sup> T<sub>RM</sub>

326 presented similar overall frequencies in vaccinated individuals when considering all functions. Of  
327 note, low percentages of SARS-CoV-2 specific CD8<sup>+</sup> T cells may be due to the use of 15-mer  
328 peptides, which are less optimal than 9/10-mer peptides for HLA class I binding <sup>3</sup>, although this is  
329 debatable <sup>21</sup>. Other methods, such as the use of activation induced markers and tetramers loaded  
330 with SARS-CoV-2 immunodominant peptides <sup>27, 30</sup> may give additional insight into the CD8<sup>+</sup> T cell  
331 response against SARS-CoV-2. Thus, considering the putative protective role of CD8<sup>+</sup> T cells  
332 observed in animal models <sup>29</sup>, further exploration of the CD8<sup>+</sup> T cell response after mRNA  
333 vaccination is warranted. our results for these vaccinated individuals are certainly encouraging.

334 We acknowledge that our study has several limitations. The small sample size for the  
335 different groups warrants further investigation with ideally larger cohorts. Finding patients that  
336 meet our inclusion criteria was however challenging and currently, patients meeting the criteria  
337 are no longer available. In addition, we addressed T cell immune responses in older and mostly  
338 oncologic patients. In general, T cell responses of cancer patients after vaccination against SARS-  
339 CoV-2 may be impaired <sup>31</sup>, which may overall underestimate immune responses in all groups of  
340 our study. However, we still detect vaccine-induced S-specific CD4<sup>+</sup> T cells in our patients, which  
341 shows that mRNA vaccination may even contribute to protection against COVID-19 in these  
342 vulnerable patients. Further, the Inf group consisted of patients recovered from mild or severe  
343 disease. Even if age and underlying conditions were similar to the other groups, disease severity  
344 may have skewed frequencies of SARS-CoV-2-specific T cells towards the higher end. Still,  
345 considering their age and condition, any of these patients with a new infection would most likely  
346 develop a more serious COVID-19 event compared to the general population. In addition, the  
347 boosted Vx3 group was sampled short term comparing to the Vx2 group, but enhancement of T  
348 cell responses would be better detected 5-10 days after boosting <sup>10, 11</sup> (which was a less likely  
349 time for scheduling surgery). Still it was enough time to suggest that there was no major  
350 enhancement of long-term durable T cell response in the lung by a third boost. Further, we did

351 not assess the contribution of T cells targeting mutation regions to the total spike since we aimed  
352 to compare the strength and function of vaccinated and naturally infected patients (these last  
353 group obtained during the first wave). However, the overall contribution of T cell responses to  
354 mutational regions/total spike responses has been reported to be low <sup>14, 32</sup>.

355 Overall, our results contribute to the understanding of disease protection mediated by  
356 current mRNA vaccines. While our data indicate a more robust and broader cellular response in  
357 convalescent patients, S-specific T cells can be detected in the lung of vaccinated individuals to  
358 similar overall levels 8 months after immunization, highlighting the durability of this immune arm.  
359 Further, while we detected increased levels of IFN $\gamma$ <sup>+</sup> T cell responses in blood after the third dose,  
360 limited benefit of boosting towards the enhancement of T cell responses in the lung was evidenced  
361 by our data. However, elderly people not responding to vaccination have been shown to benefit  
362 from a third dose <sup>23</sup> and there is an obvious benefit of boosting to provide a higher degree of  
363 antibody-mediated protection from infection in the context of high incidence of VOC <sup>1</sup>. Still, if virus  
364 neutralization is unable to completely block infection, a more robust and broader T<sub>RM</sub> response  
365 established in the lung of convalescent-infected individuals may have more chances of limiting  
366 disease. In this sense, polyfunctional CD107a<sup>+</sup> IFN $\gamma$ <sup>+</sup> cells may contribute to infection clearance  
367 or even limit the occurrence of breakthrough SARS-CoV-2 infections vaccination and absence of  
368 these cells in vaccinated patients underlines the need for the development of mucosal vaccines  
369 <sup>33</sup>, recently shown to be effective in inducing sterilizing immunity in mice <sup>34</sup>. The inclusion of other  
370 protein fragments such as nucleocapsid peptides <sup>5, 8, 19, 25, 28</sup> in combination with mucosal routes  
371 <sup>35</sup> will likely contribute to the establishment of optimal memory T cells in future vaccine strategies.

372

373

374

375

376 **Methods**

377

378 **Ethics statement**

379 This study was performed in accordance with the Declaration of Helsinki and approved by the  
380 corresponding Institutional Review Board (PR(AG)212/2020) of the Vall d'Hebron University  
381 Hospital (HUVH), Barcelona, Spain. Written informed consent was provided by all patients  
382 recruited to this study.

383

384 **Subject recruitment and sample collection**

385 Patients undergoing lung resection for various reasons at the HUVH were recruited through the  
386 Thoracic Surgery Service and invited to participate. Initially, a total of 32 patients, from whom  
387 paired blood samples and lung biopsies were collected were assayed. However, based on  
388 vaccination and/or infection status of the recruited patients, 26 (+2: HL174 and HL162) patients  
389 were finally included. Supplemental Table 1 summarizes relevant information from included  
390 patients. For all participants, whole blood was collected with EDTA anticoagulant. Plasma was  
391 collected and stored at  $-80^{\circ}\text{C}$  (except for 4 patients distributed among the different groups, as  
392 indicated in Supplemental Table 1, for which this sample was not available) and PBMCs were  
393 isolated via Ficoll–Paque separation and processed immediately for stimulation assays.

394

395 **Phenotyping and Intracellular Cytokine Staining of lung biopsies**

396 Immediately following surgery, healthy areas from patients undergoing lung resection were  
397 collected in antibiotic-containing RPMI 1640 medium and processed as published<sup>8</sup>. Briefly, 8-mm<sup>3</sup>  
398 dissected blocks were first enzymatically digested with 5 mg/ml collagenase IV (Gibco) and  
399 100µg/ml of DNase I (Roche) for 30 min at 37 °C and 400 rpm and, then, mechanically digested  
400 with a pestle. The resulting cellular suspension was first filtered through a 70µm pore size cell  
401 strainer and then filtered through a 30µm pore size cell strainer (Labclinics). After washing with



402 PBS, cells were stimulated in a 96-well round-bottom plate for 16 to 18 hours at 37°C with 1µg/mL  
403 of SARS-CoV-2 peptides (PepTivator SARS-CoV-2 M, N or S, Miltenyi Biotec) in the presence of  
404 3.3µL/mL α-CD28/CD49d (clones L293 and L25), 0.55µL/mL Brefeldin A, 0.385µL/mL Monensin  
405 and 5 µL/100µL anti-CD107a-PE-Cy5 (all from BD Biosciences). For each patient, a negative  
406 control, cells treated with medium, and positive control, cells incubated in the presence of 0.4nM  
407 PMA and 20µM Ionomycin, were included. Next day, cellular suspensions were stained with  
408 Live/Dead Aqua (Invitrogen) and anti-CD103 (FITC, Biolegend), anti-CD69 (PE-CF594, BD  
409 Biosciences), anti-CD40 (APC-Cy7, Biolegend), anti-CD8 (APC, BD Biosciences), anti-CD3  
410 (BV650, BD Biosciences) and anti-CD45 (BV605, BD Biosciences) antibodies. Cells were  
411 subsequently fixed and permeabilized using the FoxP3 Fix/Perm kit (BD Biosciences) and stained  
412 with anti-IL-4 (PE-Cy7, eBioscience), anti-IL-10 (PE, BD Biosciences), anti-T-bet (BV421,  
413 Biolegend) and anti-IFN $\gamma$  (AF700, Invitrogen) antibodies. After fixation with PBS 2% PFA, cells  
414 were acquired in a BD LSR Fortessa flow cytometer (Cytomics Platform, High Technology Unit,  
415 Vall d'Hebron Institut de Recerca).

416

#### 417 **Phenotyping and Intracellular Cytokine Staining in blood**

418 Freshly isolated PBMCs were labelled for CCR7 (PE-CF594, BD Biosciences) and CXCR3  
419 (BV650, BD Biosciences) for 30 min at 37°C. After washing with PBS, PBMCs were stimulated in  
420 a 96-well round-bottom plate for 16 to 18 hours at 37°C with 1µg/mL of SARS-CoV-2 peptides  
421 together with the same concentration of Brefeldin A, Monensin, α-CD28/CD49d and CD107a-PE-  
422 Cy5, as stated for the lung suspension above and published before<sup>8</sup>. For each patient, a negative  
423 control and a positive control were also included. After stimulation, cells were washed twice with  
424 PBS and stained with Aqua LIVE/DEAD fixable dead cell stain kit (Invitrogen). Cell surface  
425 antibody staining included anti-CD3 (Per-CP), anti-CD4 (BV605) and anti-CD56 (FITC) (all from  
426 BD Biosciences). Cells were subsequently fixed and permeabilized using the Cytofix/Cytoperm

427 kit (BD Biosciences) and stained with anti-Caspase-3 (AF647, BD Biosciences), anti-Bcl-2  
428 (BV421, Biolegend), anti-IL-4 (PE-Cy7, eBioscience), anti-IL-10 (PE, BD Biosciences) and anti-  
429 IFN $\gamma$  (AF700, Invitrogen) for 30 mins. Cells were then fixed with PBS 2% PFA and acquired in a  
430 BD LSR Fortessa flow cytometer.

431

### 432 **SARS-CoV-2 serology**

433 The serological status of patients included in this study was determined in serum samples using  
434 two commercial chemiluminescence immunoassays (CLIA) targeting specific SARS-CoV-2  
435 antibodies: (1) Elecsys Anti-SARS-CoV-2 (Roche Diagnostics, Mannheim, Germany) was  
436 performed on the Cobas 8800 system (Roche Diagnostics, Basel, Switzerland) for the  
437 determination of total antibodies (including IgG, IgM, and IgA) against nucleocapsid (N) SARS-  
438 CoV-2 protein; and (2) Liaison SARS-CoV-2 TrimericS IgG (DiaSorin, Stillwater, MN) was  
439 performed on the LIAISON XL Analyzer (DiaSorin, Saluggia, Italy) for the determination of IgG  
440 antibodies against the spike (S) glycoprotein.

441

### 442 **Pseudovirus neutralization assay**

443 The spike of the Omicron SARS-CoV-2 was generated (GeneArt Gene Synthesis, ThermoFisher  
444 Scientific) from the plasmid containing the D614G mutation with a deletion of 19 amino acids,  
445 which was modified to include the mutations specific for this VOC (A67V,  $\Delta$ 69-70, T95I,  
446 G142D/ $\Delta$ 143-145,  $\Delta$ 211/L212I, ins214EPE, G339D, S371L, S373P, S375F, K417N, N440K,  
447 G446S, S477N, T478K, E484A, Q493R, G496S, Q498R, N501Y, Y505H, T547K, D614G, H655Y,  
448 N679K, P681H, N764K, D796Y, N856K, Q954H, N969K, L981F) (kindly provided by Drs. J.  
449 Blanco and B. Trinite). Pseudotyped viral stocks of VSV\* $\Delta$ G(Luc)-S were generated following the  
450 protocol described in<sup>36</sup>. Briefly, 293T cells were transfected with 3 $\mu$ g of the omicron plasmid  
451 (pcDNA3.1 omicron). Next day, cells were infected with a VSV-G-Luc virus (MOI=1) for 2h and  
452 washed twice with warm PBS. To neutralize contaminating VSV\* $\Delta$ G(Luc)-G particles cells were

453 incubated overnight in media containing 10% of the supernatant from the I1 hybridoma (ATCC  
454 CRL-2700), containing anti-VSV-G antibodies. Next day, viral particles were harvested and  
455 titrated in VeroE6 cells by enzyme luminescence assay (Britelite plus kit; PerkinElmer). For the  
456 neutralization assays, VeroE6 cells were seeded in 96-well white, flat-bottom plates (Thermo  
457 Scientific) at 30,000 cells/well. Plasma samples were heat-inactivated and diluted four-fold  
458 towards a concentration of 1/32 of the initial sample. Diluted plasma samples were then incubated  
459 with pseudotyped virus (VSV\* $\Delta$ G(Luc)-S<sup>omicron</sup>) with titers of approximately  $1 \times 10^6 - 5 \times 10^5$  RLU/ml  
460 of luciferase activity - in a 96 well-plate flat bottom for 1 hour at 37°C, 5% CO<sub>2</sub>. Next, 30,000 Vero  
461 E6 cells were added to each well and incubated at 37°C, 5% CO<sub>2</sub> for 20-24 hours. Then, viral  
462 entry was measured by the expression of luciferase. Cells were incubated with Britelite plus  
463 reagent (Britelite plus kit; PerkinElmer) and then transferred to an opaque black plate.  
464 Luminescence was immediately recorded by a luminescence plate reader (LUMIstar Omega).  
465 Viral neutralization was calculated as the reciprocal plasma dilution (ID<sub>50</sub>) resulting in a 50%  
466 reduction in relative light units. If no neutralization was observed, an arbitrary titer value of 16 (half  
467 of the limit of detection [LOD]) was reported.

468

#### 469 **Statistical analyses**

470 Flow cytometry data was analyzed using FlowJo v10.7.1 software (TreeStar). Data and statistical  
471 analyses were performed using Prism 8.0 (GraphPad Software, La Jolla, CA, USA). Data shown  
472 in bar graphs were expressed as median and Interquartile range (IQR), unless stated otherwise.  
473 Correlation analyses were performed using non-parametric Spearman rank correlation. Kruskal-  
474 Wallis rank-sum test with Dunn's post-hoc test was used for multiple comparisons. Friedmann  
475 test with Dunn's post-hoc test was applied for paired comparisons. A *P* value <0.05 was  
476 considered statistically significant. Antigen-specific T-cell data was calculated as the net  
477 frequency, where the individual percentage of expression for a given molecule in the control

478 condition (vehicle) was subtracted from the corresponding SARS-CoV-2-peptide stimulated  
479 conditions.

480

#### 481 **Data availability**

482 The data that support the findings of this study are available from the corresponding author upon  
483 reasonable request.

#### **References**

- 484 1. Cromer D, *et al.* Neutralising antibody titres as predictors of protection against  
485 SARS-CoV-2 variants and the impact of boosting: a meta-analysis. *The Lancet*  
486 *Microbe* **3**, e52-e61 (2022).  
487
- 488 2. Geers D, *et al.* SARS-CoV-2 variants of concern partially escape humoral but not  
489 T-cell responses in COVID-19 convalescent donors and vaccinees. *Science*  
490 *immunology* **6**, (2021).  
491
- 492 3. Keeton R, *et al.* T cell responses to SARS-CoV-2 spike cross-recognize  
493 Omicron. *Nature* **603**, 488-492 (2022).  
494
- 495 4. Moss P. The T cell immune response against SARS-CoV-2. *Nat Immunol* **23**,  
496 186-193 (2022).  
497

- 498 5. Kundu R, *et al.* Cross-reactive memory T cells associate with protection against  
499 SARS-CoV-2 infection in COVID-19 contacts. *Nature communications* **13**, 80  
500 (2022).  
501
- 502 6. Niessl J, Sekine T, Buggert M. T cell immunity to SARS-CoV-2. *Seminars in*  
503 *immunology* **55**, 101505 (2021).  
504
- 505 7. Jung JH, *et al.* SARS-CoV-2-specific T cell memory is sustained in COVID-19  
506 convalescent patients for 10 months with successful development of stem cell-  
507 like memory T cells. *Nature communications* **12**, 4043 (2021).  
508
- 509 8. Grau-Exposito J, *et al.* Peripheral and lung resident memory T cell responses  
510 against SARS-CoV-2. *Nature communications* **12**, 3010 (2021).  
511
- 512 9. Szabo PA, *et al.* Longitudinal profiling of respiratory and systemic immune  
513 responses reveals myeloid cell-driven lung inflammation in severe COVID-19.  
514 *Immunity* **54**, 797-814 e796 (2021).  
515
- 516 10. Goel RR, *et al.* mRNA vaccines induce durable immune memory to SARS-CoV-2  
517 and variants of concern. *Science* **374**, abm0829 (2021).  
518
- 519 11. Zhang Z, *et al.* Humoral and cellular immune memory to four COVID-19  
520 vaccines. *bioRxiv : the preprint server for biology*, (2022).

- 521
- 522 12. Ortega N, *et al.* Seven-month kinetics of SARS-CoV-2 antibodies and role of pre-  
523 existing antibodies to human coronaviruses. *Nature communications* **12**, 4740  
524 (2021).
- 525
- 526 13. Laidlaw BJ, *et al.* CD4+ T cell help guides formation of CD103+ lung-resident  
527 memory CD8+ T cells during influenza viral infection. *Immunity* **41**, 633-645  
528 (2014).
- 529
- 530 14. Minervina AA, *et al.* SARS-CoV-2 antigen exposure history shapes phenotypes  
531 and specificity of memory CD8 T cells. *medRxiv : the preprint server for health*  
532 *sciences*, (2022).
- 533
- 534 15. Sheikh-Mohamed S, *et al.* Systemic and mucosal IgA responses are variably  
535 induced in response to SARS-CoV-2 mRNA vaccination and are associated with  
536 protection against subsequent infection. *Mucosal immunology*, (2022).
- 537
- 538 16. Hassan AO, *et al.* A Single-Dose Intranasal ChAd Vaccine Protects Upper and  
539 Lower Respiratory Tracts against SARS-CoV-2. *Cell* **183**, 169-184 e113 (2020).
- 540
- 541 17. Le Bert N, *et al.* Highly functional virus-specific cellular immune response in  
542 asymptomatic SARS-CoV-2 infection. *The Journal of experimental medicine* **218**,  
543 (2021).

544

545 18. Grifoni A, *et al.* Targets of T Cell Responses to SARS-CoV-2 Coronavirus in  
546 Humans with COVID-19 Disease and Unexposed Individuals. *Cell* **181**, 1489-  
547 1501 e1415 (2020).

548

549 19. Taus E, *et al.* Dominant CD8(+) T Cell Nucleocapsid Targeting in SARS-CoV-2  
550 Infection and Broad Spike Targeting From Vaccination. *Front Immunol* **13**,  
551 835830 (2022).

552

553 20. Demaret J, *et al.* Severe SARS-CoV-2 patients develop a higher specific T-cell  
554 response. *Clinical & translational immunology* **9**, e1217 (2020).

555

556 21. Thieme CJ, *et al.* Robust T Cell Response Toward Spike, Membrane, and  
557 Nucleocapsid SARS-CoV-2 Proteins Is Not Associated with Recovery in Critical  
558 COVID-19 Patients. *Cell reports Medicine* **1**, 100092 (2020).

559

560 22. Poon MML, *et al.* Heterogeneity of human anti-viral immunity shaped by virus,  
561 tissue, age, and sex. *Cell reports* **37**, 110071 (2021).

562

563 23. Romero-Olmedo AJ, *et al.* Induction of robust cellular and humoral immunity  
564 against SARS-CoV-2 after a third dose of BNT162b2 vaccine in previously  
565 unresponsive older adults. *Nature microbiology* **7**, 195-199 (2022).

566

- 567 24. Matchett WE, *et al.* Cutting Edge: Nucleocapsid Vaccine Elicits Spike-  
568 Independent SARS-CoV-2 Protective Immunity. *Journal of immunology* **207**, 376-  
569 379 (2021).  
570
- 571 25. Peng Y, *et al.* An immunodominant NP105-113-B\*07:02 cytotoxic T cell response  
572 controls viral replication and is associated with less severe COVID-19 disease.  
573 *Nat Immunol* **23**, 50-61 (2022).  
574
- 575 26. Braun J, *et al.* SARS-CoV-2-reactive T cells in healthy donors and patients with  
576 COVID-19. *Nature*, (2020).  
577
- 578 27. Niessl J, *et al.* Identification of resident memory CD8(+) T cells with functional  
579 specificity for SARS-CoV-2 in unexposed oropharyngeal lymphoid tissue. *Sci*  
580 *Immunol* **6**, eabk0894 (2021).  
581
- 582 28. Mazzoni A, *et al.* First-dose mRNA vaccination is sufficient to reactivate  
583 immunological memory to SARS-CoV-2 in subjects who have recovered from  
584 COVID-19. *The Journal of clinical investigation* **131**, (2021).  
585
- 586 29. Channappanavar R, Zhao J, Perlman S. T cell-mediated immune response to  
587 respiratory coronaviruses. *Immunologic research* **59**, 118-128 (2014).  
588



- 589 30. Saini SK, *et al.* SARS-CoV-2 genome-wide T cell epitope mapping reveals  
590 immunodominance and substantial CD8(+) T cell activation in COVID-19  
591 patients. *Sci Immunol* **6**, (2021).  
592
- 593 31. Fendler A, *et al.* COVID-19 vaccines in patients with cancer: immunogenicity,  
594 efficacy and safety. *Nat Rev Clin Oncol* **19**, 385-401 (2022).  
595
- 596 32. Skelly DT, *et al.* Two doses of SARS-CoV-2 vaccination induce robust immune  
597 responses to emerging SARS-CoV-2 variants of concern. *Nature*  
598 *communications* **12**, 5061 (2021).  
599
- 600 33. Topol EJ, Iwasaki A. Operation Nasal Vaccine-Lightning speed to counter  
601 COVID-19. *Sci Immunol*, eadd9947 (2022).  
602
- 603 34. Tang J, *et al.* Respiratory mucosal immunity against SARS-CoV-2 following  
604 mRNA vaccination. *Sci Immunol*, eadd4853 (2022).  
605
- 606 35. Mao T, *et al.* Unadjuvanted intranasal spike vaccine booster elicits robust  
607 protective mucosal immunity against sarbecoviruses. *bioRxiv : the preprint server*  
608 *for biology*, (2022).  
609
- 610 36. Grau-Exposito J, *et al.* Evaluation of SARS-CoV-2 entry, inflammation and new  
611 therapeutics in human lung tissue cells. *PLoS pathogens* **18**, e1010171 (2022).  
612

613 **Author contributions**

614 Conceptualization, M.G.; Patient Recruitment and Sample Collection, J.R., V.F.; Methodology,  
615 DKJ.P., SG.K., A.G.R., J.R-C, C.M., J.E.; Investigation, DKJ.P., SG.K., A.G.R., J.E.; Formal  
616 Analysis, DKJ.P., A.G.R., M.J.B. and M.G.; Writing-Original Draft, DKJ.P. and M.G; Writing-  
617 Review & Editing, all authors; Funding Acquisition, M.G.; Supervision, M.G.

618

619 **Acknowledgements**

620 We would like to thank all the patients who participated in the study and Drs. Julià Blanco and  
621 Benjamin Trinite for providing the plasmid encoding the omicron spike. This work was supported  
622 by grants from Fundació La Marató TV3 (201814-10 FMTV3 and 202112-30 FMTV3), from the  
623 Health department of the Government of Catalonia (DGRIS 1\_5), and the Spanish AIDS network  
624 Red Temática Cooperativa de Investigación en SIDA (RD16/0025/0007). M.J.B is supported by  
625 the Miguel Servet program funded by the Spanish Health Institute Carlos III (CP17/00179). The  
626 funders had no role in study design, data collection and analysis, the decision to publish, or  
627 preparation of the manuscript.

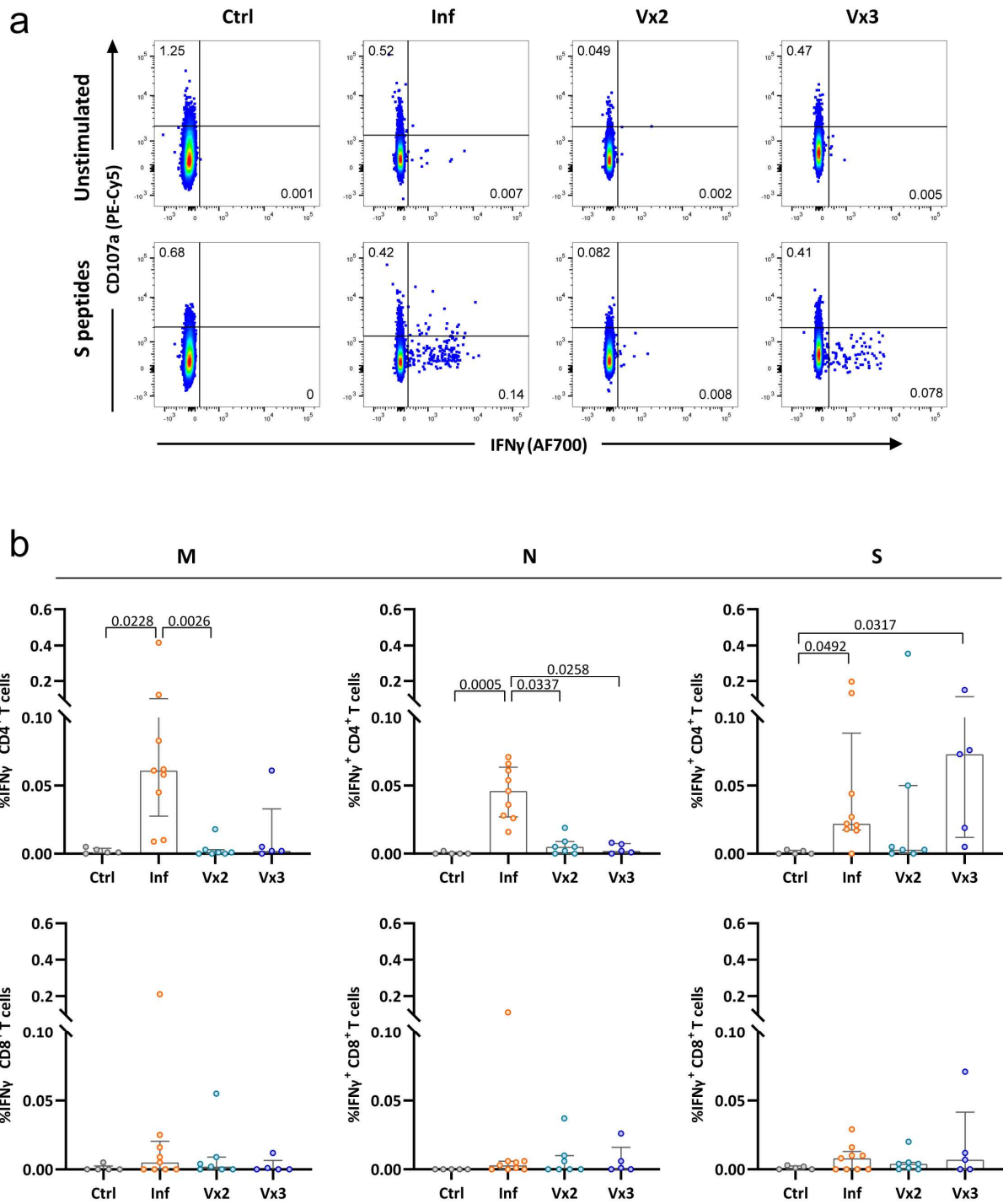
**Competing interests**

The authors declare no competing interests.

628

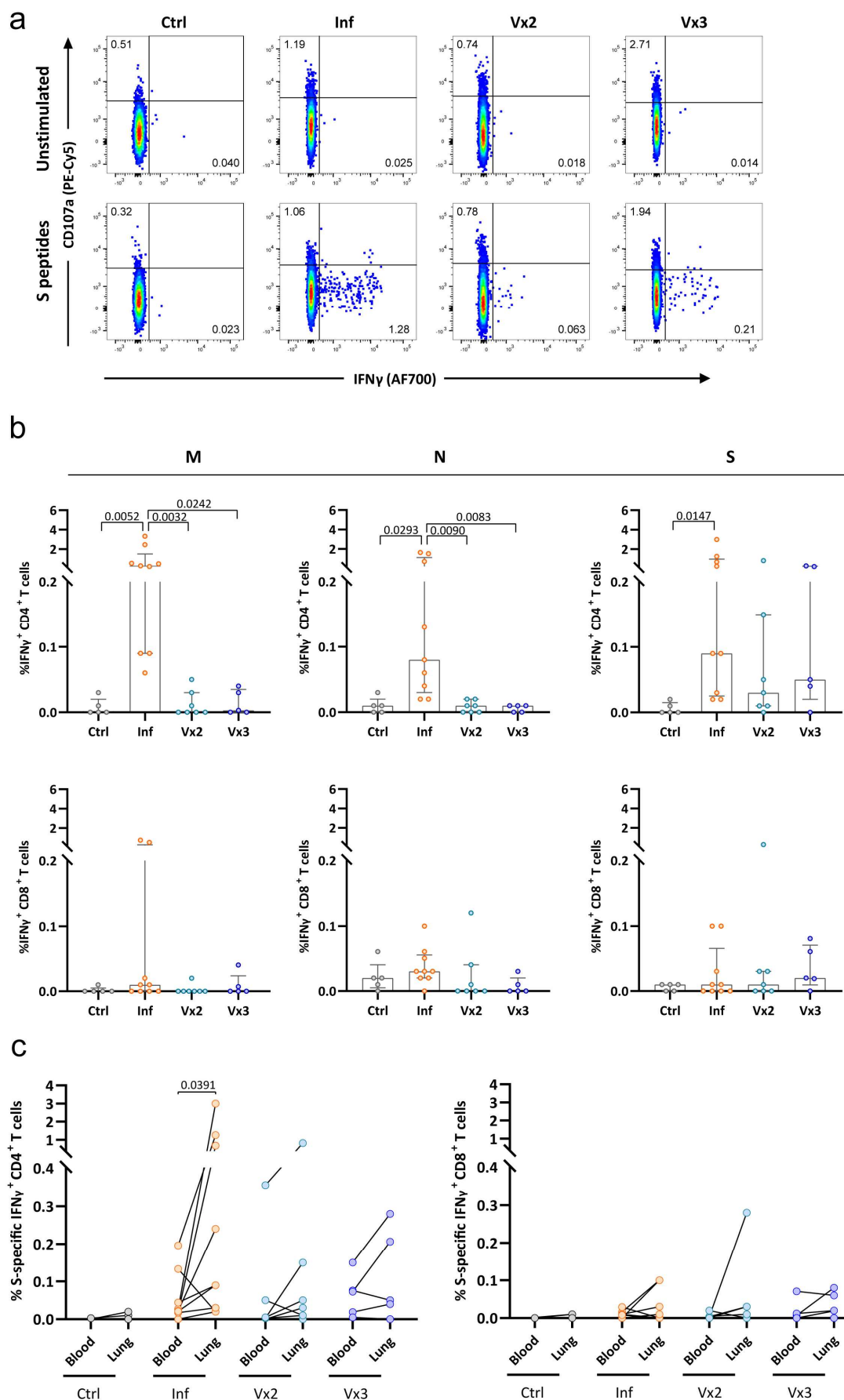
629 FIGURES AND FIGURE LEGENDS

630 Figure 1



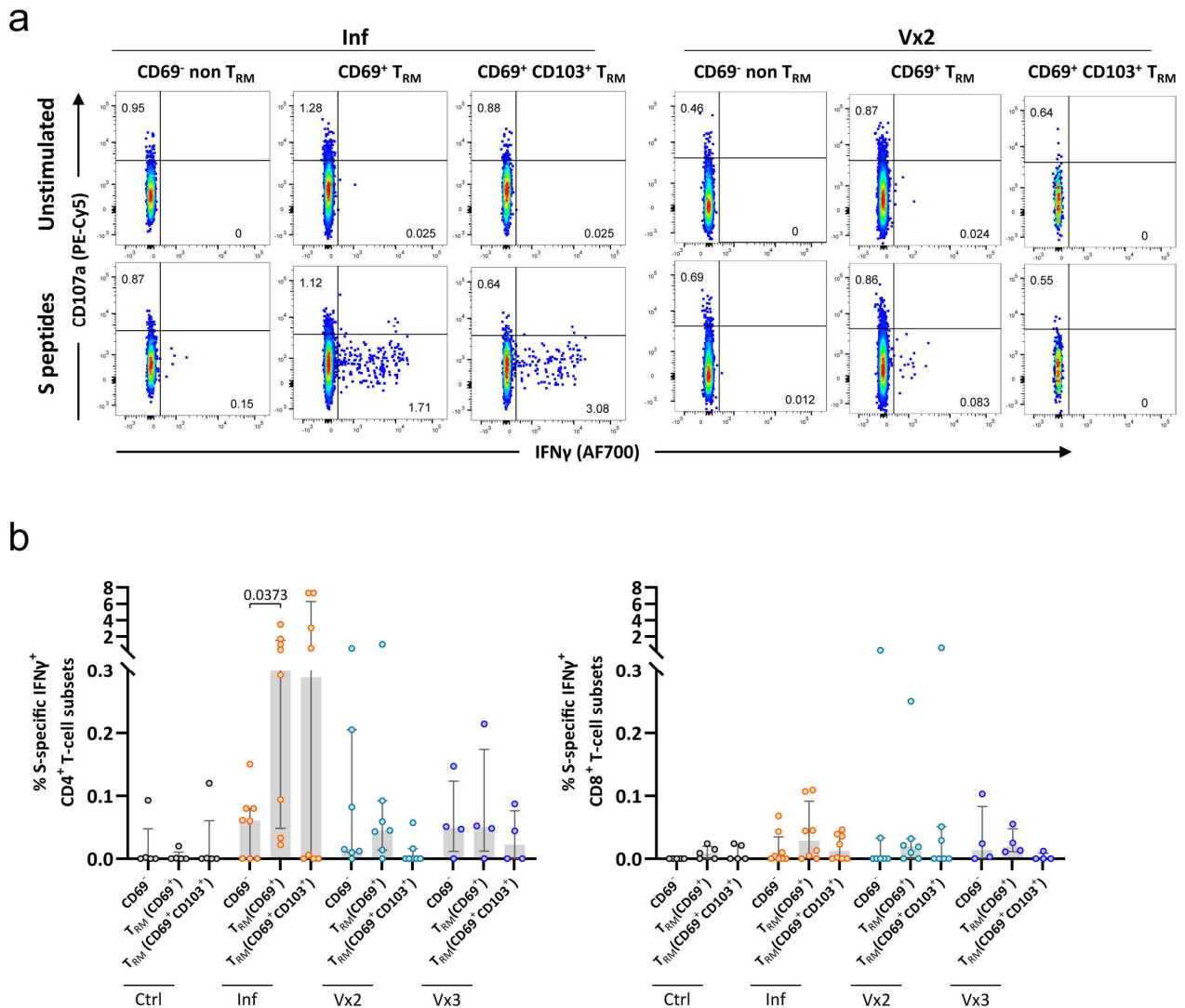
631 **Figure 1. SARS-CoV-2-specific T-cell responses in peripheral blood from convalescent and**  
632 **vaccinated patients. (A)** Representative flow-cytometry plots showing CD4<sup>+</sup> T cells expressing  
633 CD107a and IFN $\gamma$  after exposure of whole PBMCs to S-peptide pools or left unstimulated for each  
634 of the four groups included in this study (complete gating strategy is shown in Supplemental  
635 Figure 2A). **(B)** Comparison of the net frequency (background subtracted) of IFN $\gamma$ <sup>+</sup> cells within  
636 CD4<sup>+</sup> (upper) and CD8<sup>+</sup> (lower) T-cell subsets after stimulation of PBMCs with any of the three  
637 viral peptide pools (membrane (M), nucleocapsid (N) and spike (S) peptides). Data are shown as  
638 median  $\pm$  IQR, where each dot represents an individual patient for each group (Ctrl, control, n=5;  
639 Inf, convalescent infected, n=9; Vx2, vaccine 2 doses, n=7 and Vx3, vaccine 3 doses, n=5).  
640 Statistical significance was determined by Kruskal-Wallis test (with Dunn's post-test).

641 **Figure 2**



642 **Figure 2. SARS-CoV-2-specific lung T-cell responses from convalescent and vaccinated**  
643 **patients and comparison between tissue compartments. (A)** Representative flow-cytometry  
644 plots showing CD4<sup>+</sup> T cells expressing CD107a and IFN $\gamma$  after exposure of single-cell  
645 suspensions of lung tissue to S-peptide pools or left unstimulated for each of the four groups  
646 included in this study (complete gating strategy is shown in Supplemental Figure 2B). **(B)**  
647 Comparison of the net frequency (background subtracted) of IFN $\gamma$ <sup>+</sup> cells within CD4<sup>+</sup> (upper) and  
648 CD8<sup>+</sup> (lower) T-cell subsets after exposure of lung single-cell suspensions to any of the three viral  
649 peptide pools (membrane (M), nucleocapsid (N) and spike (S) peptides). **(C)** Comparison of the  
650 net frequency of IFN $\gamma$ <sup>+</sup> cells within CD4<sup>+</sup> (left) and CD8<sup>+</sup> (right) T-cell subsets in paired blood and  
651 lung samples of each group after exposure to S-peptide pools. Data in bar graphs are shown as  
652 median  $\pm$  IQR, where each dot represents an individual patient for each group (Ctrl, control, n=5;  
653 Inf, convalescent infected, n=9; Vx2, vaccine 2 doses, n=7 and Vx3, vaccine 3 doses, n=5).  
654 Statistical significance was determined by **(B)** Kruskal-Wallis test (with Dunn's post-test) or **(C)**  
655 Friedmann test (with Dunn's post-test).  
656

657 **Figure 3**



658

659 **Figure 3. Frequency of Spike-specific  $T_{RM}$  cells in the lung. (A)** Representative flow-cytometry

660 plots showing three subsets of  $CD4^+$  T cells present in the lung:  $CD69^-$  non- $T_{RM}$ ,  $CD69^+$   $T_{RM}$ , and

661  $CD69^+CD103^+$   $T_{RM}$  cells expressing  $CD107a$  and  $IFN\gamma$  after exposure of single-cell suspensions

662 of lung tissue to S-peptide pools or left unstimulated for an Inf and a Vx2 patients. (B) Comparison

663 of the net frequency of S-specific  $IFN\gamma^+$  cells within the three (non-)  $T_{RM}$  cell subsets present in

664 the lung for each group. Data in bar graphs are shown as median  $\pm$  IQR, where each dot

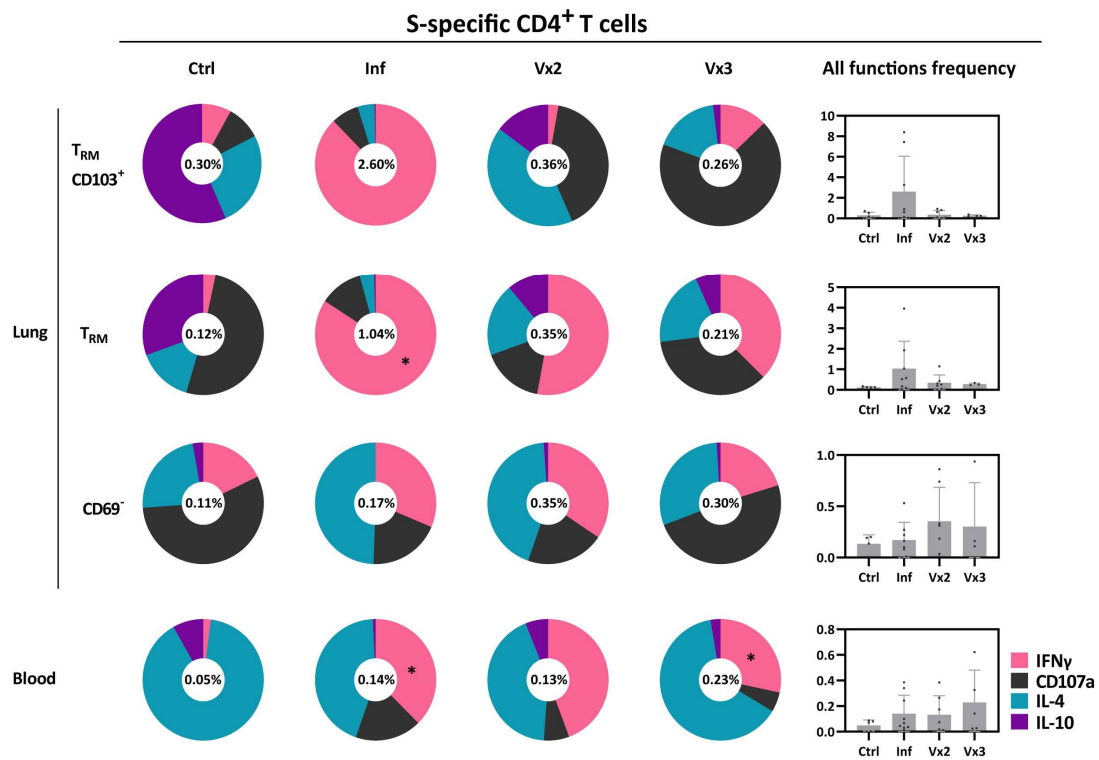
665 represents an individual patient for each group (Ctrl, control, n=5; Inf, convalescent infected, n=8;

666 Vx2, vaccine 2 doses, n=7 and Vx3, vaccine 3 doses, n=4). Statistical significance was  
667 determined by Friedmann test (with Dunn's post-test) for the difference between the cellular  
668 subsets within each patient group.

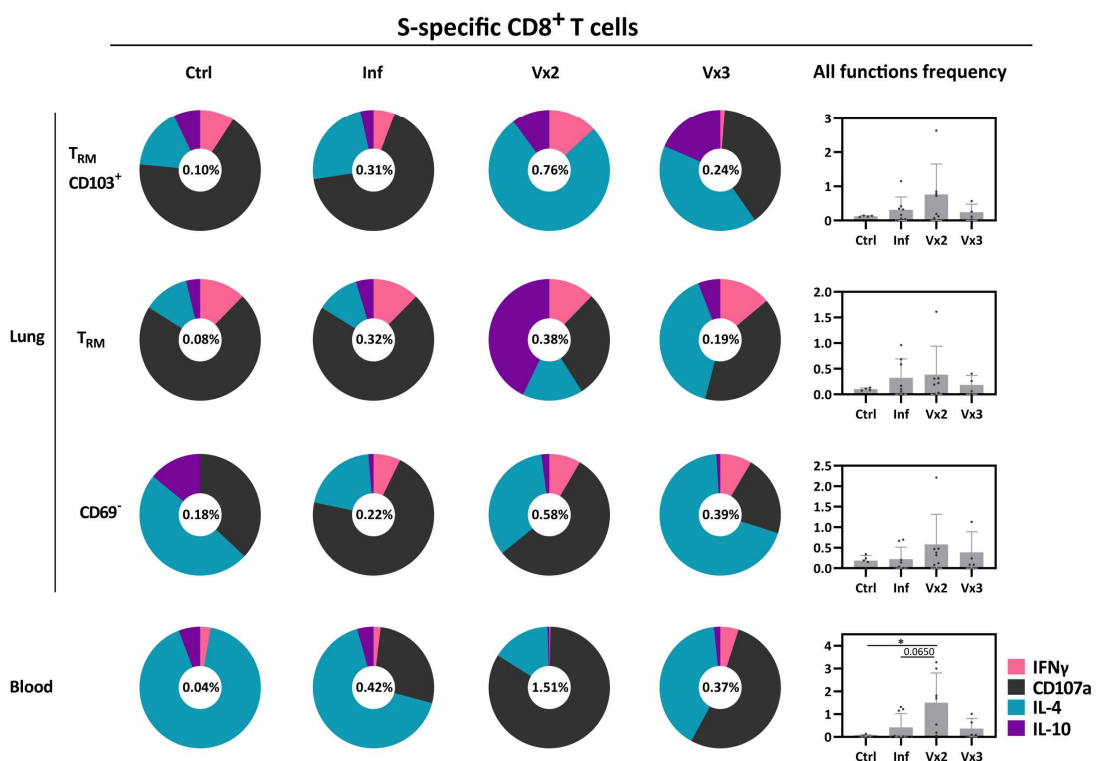


669 **Figure 4**

**a**



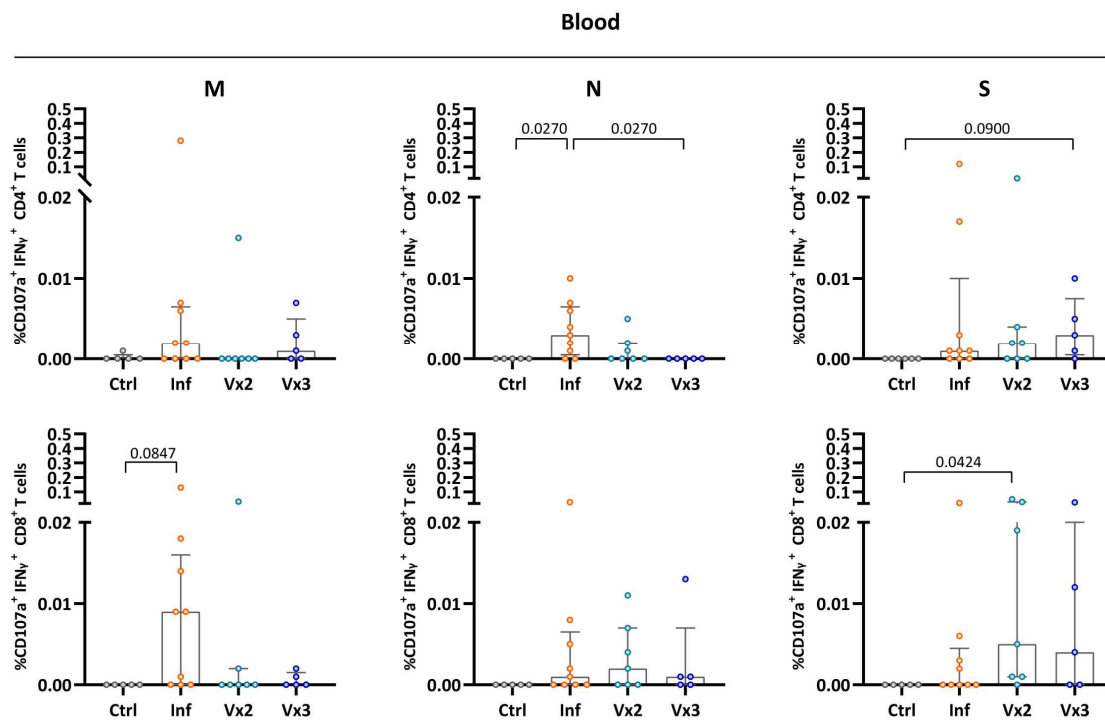
**b**



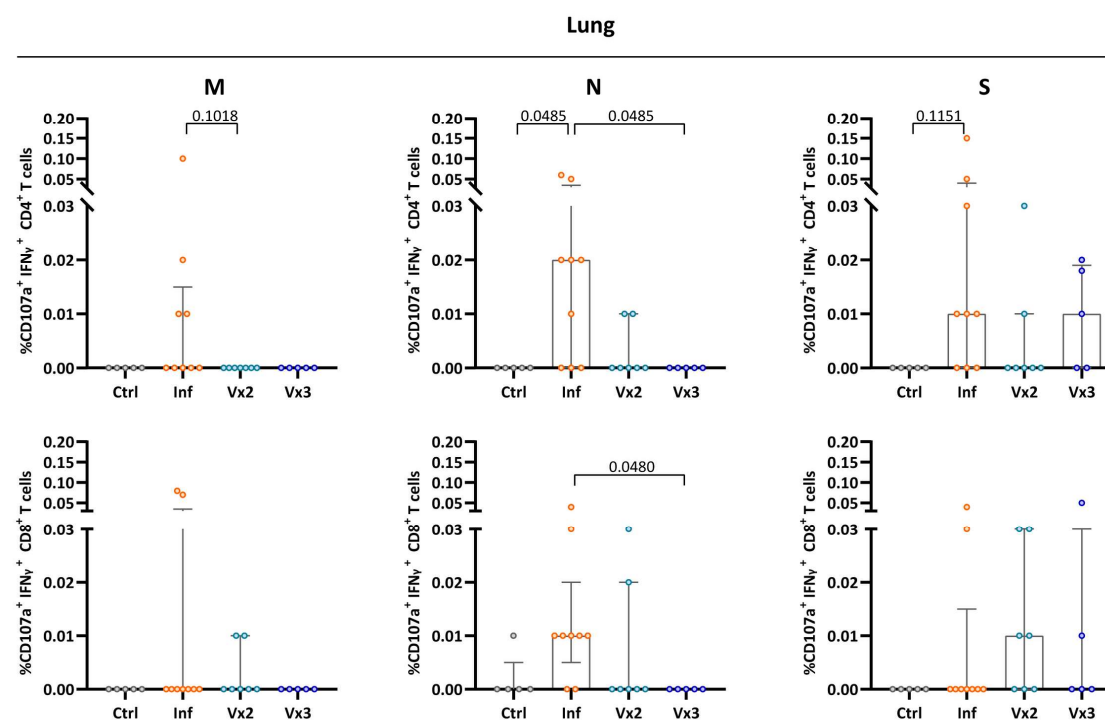
670 **Figure 4. Overall functional T-cell response of lung and blood compartments. (A, B)** Donut  
671 charts displaying the net contribution of each functional marker (IFN $\gamma$ , CD107a, IL-4, and IL-10)  
672 to the overall S-specific CD4<sup>+</sup> (A) and CD8<sup>+</sup> (B) T-cell response within the lung resident and non-  
673 resident T-cell subsets and in peripheral blood for each of the individual patient groups. Data  
674 represent the mean value of the net frequency of each function within the patient group, including  
675 both responders and non-responders. The frequency shown inside each donut chart represents  
676 the accumulated mean response of all functions. Bar charts on the right show the mean of the  
677 total frequency considering all functions per group (mean  $\pm$  SD). Statistical significance was  
678 determined by Kruskal-Wallis test (with Dunn's post-test) for the difference between each group.  
679 \*  $P < 0.05$ .

680 **Figure 5**

**a**

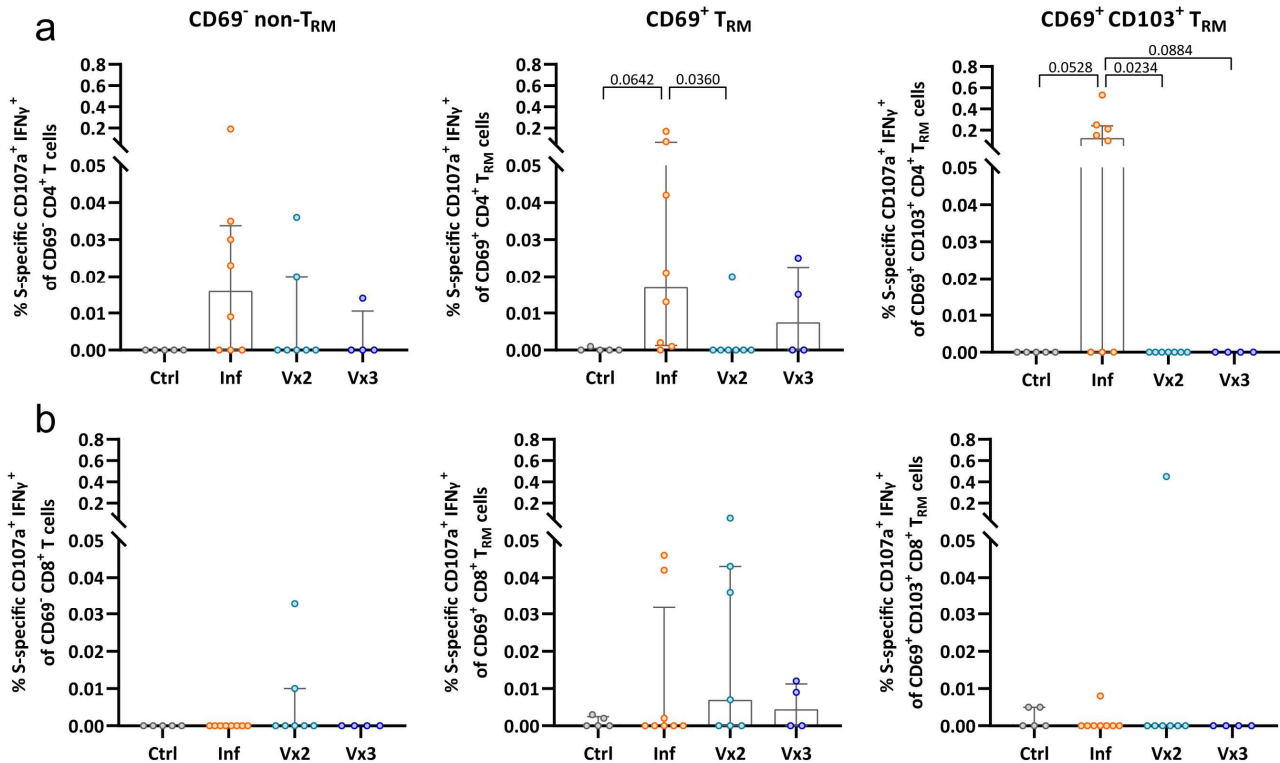


**b**



681 **Figure 5. Polyfunctional CD4<sup>+</sup> and CD8<sup>+</sup> T-cell responses in blood and lung of convalescent**  
682 **and vaccinated patients. (A, B)** Comparison of the net frequency of polyfunctional CD107a<sup>+</sup>  
683 IFN $\gamma$ <sup>+</sup> cells within CD4<sup>+</sup> and CD8<sup>+</sup> T-cell subsets for each of the four groups after exposure of  
684 PBMCs (A) or single-cell suspensions of lung tissue (B) to any of the three viral peptide pools  
685 (membrane (M), nucleocapsid (N) and spike (S) peptides). Data in bar graphs are shown as  
686 median  $\pm$  IQR, where each dot represents an individual patient for each group (Ctrl, control, n=5;  
687 Inf, convalescent infected, n=9; Vx2, vaccine 2 doses, n=7 and Vx3, vaccine 3 doses, n=5).  
688 Statistical significance was determined by was determined using Kruskal-Wallis test (with Dunn's  
689 post-test).  
690  
691  
692  
693

694 **Figure 6**



695

696 **Figure 6. Frequency of polyfunctional T-cell responses against spike with a tissue-resident**

697 **phenotype in the lung.** Comparison of the net frequency of S-specific polyfunctional CD107a<sup>+</sup>

698 IFN $\gamma$ <sup>+</sup> cells within lung CD4<sup>+</sup> (upper) and CD8<sup>+</sup> (lower) (non-) tissue-resident cell subsets (CD69-

699 non-T<sub>RM</sub>, CD69<sup>+</sup> T<sub>RM</sub>, and CD69<sup>+</sup>CD103<sup>+</sup> T<sub>RM</sub> cells) for each of the four patient groups after

700 exposure of single-cell lung suspensions to S-peptide pools. Data in bar graphs are shown as

701 median  $\pm$  IQR, where each dot represents an individual patient for each group (Ctrl, control, n=5;

702 Inf, convalescent infected, n=8; Vx2, vaccine 2 doses, n=7 and Vx3, vaccine 3 doses, n=4).

703 Statistical significance was determined by Kruskal-Wallis test (with Dunn's post-test) for the

704 difference between the groups.